In the format provided by the authors and unedited.

An aberrant SREBP-dependent lipogenic program promotes metastatic prostate cancer

Ming Chen[1], Jiangwen Zhang[2], Katia Sampieri[1,10], John G. Clohessy[1,3], Lourdes Mendez[1], Enrique Gonzalez-Billalabeitia[1], Xue-Song Liu[1], Yu-Ru Lee[1], Jacqueline Fung[1], Jesse M. Katon[1], Archita Venugopal Menon[1], Kaitlyn A. Webster[1], Christopher Ng[1], Maria Dilia Palumbieri[1], Moussa S. Diolombi[1], Susanne B. Breitkopf[4], Julie Teruya-Feldstein[5,11], Sabina Signoretti[6], Roderick T. Bronson[7], John M. Asara[4], Mireia Castillo-Martin[8,9], Carlos Cordon-Cardo [8] and Pier Paolo Pandolfi [1]*

[1]Cancer Research Institute, Beth Israel Deaconess Cancer Center, Department of Medicine and Pathology, Beth Israel Deaconess Medical Center, Harvard Medical School, Boston, MA, USA. [2]School of Biological Sciences, University of Hong Kong, Hong Kong, China. [3]Preclinical Murine Pharmacogenetics Facility and Mouse Hospital, Beth Israel Deaconess Medical Center, Harvard Medical School, Boston, MA, USA. [4]Division of Signal Transduction, Beth Israel Deaconess Medical Center and Department of Medicine, Harvard Medical School, Boston, MA, USA. [5]Department of Pathology, Sloan-Kettering Institute, Memorial Sloan-Kettering Cancer Center, New York, NY, USA. [6]Department of Pathology, Brigham and Women's Hospital and Harvard Medical School, Boston, MA, USA. [7]Department of Microbiology and Immunobiology, Harvard Medical School, Boston, MA, USA. [8]Department of Pathology, Icahn School of Medicine at Mount Sinai, New York, NY, USA. [9]Department of Pathology, Champalimaud Center for the Unknown, Lisbon, Portugal. Present address: [10]GSK Vaccines, Antigen Identification and Molecular Biology, Siena, Italy. [11]Department of Pathology, Icahn School of Medicine at Mount Sinai, New York, NY, USA. *e-mail: ppandolf@bidmc.harvard.edu
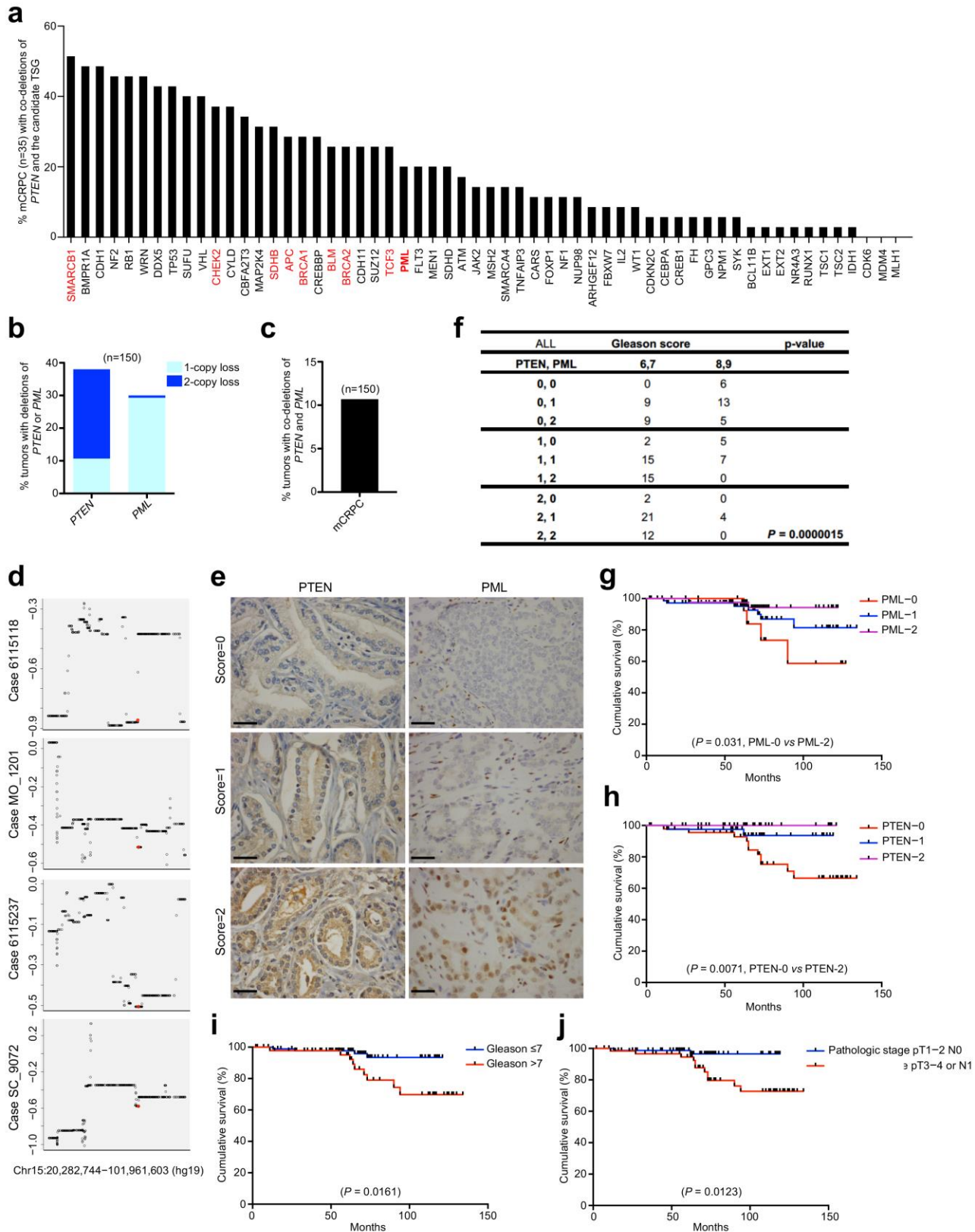
Supplementary Figure 1

Co-loss of PTEN and PML expression in advanced and metastatic human CaP

(**a**) Bar graph showing the percentage of co-deletion of *PTEN* with 58 high-confidence TSGs[32] in the Grasso *et al.* dataset of the mCRPC samples[14], respectively (4 out of 62 TSGs from the Walker *et al* gene list, data not available). The genes co-deleted with *PTEN* only in metastatic disease among the top 25 TSGs are highlighted in Red. (**b,c**) Bar graph showing the percentage of deletion of *PTEN or PML* (**b**), or *PTEN* and *PML* (**c**) in mCRPC samples from the Robinson *et al.* dataset[25]. (**d**) Representative homozygous or hemizygous focal *PML* deletion from the Robinson *et al.* dataset (38% (17/45) of PML deletion was focal)[25]. Copy number plots with x-axis representing chromosomal 15q and y-axis referring to copy number level. Red open circle indicates genomic position of *PML*. (**e**) Representative IHC staining of PTEN or PML showing examples of low, medium and high staining. Scale bar, 50μm. (**f**) Table showing the significant correlation of co-loss of PTEN and PML protein expression during the disease progression. The number of cases in each expression category was listed together with Gleason score. (**g-j**) Overall survival curves for CaP patients after radical prostatectomy based on the expression of PML protein (**g**), the expression of PTEN protein (**h**), Gleason score (**i**), or pathologic stage (**j**). In **f**, Pearson's chi-squared test was used to determine significance.
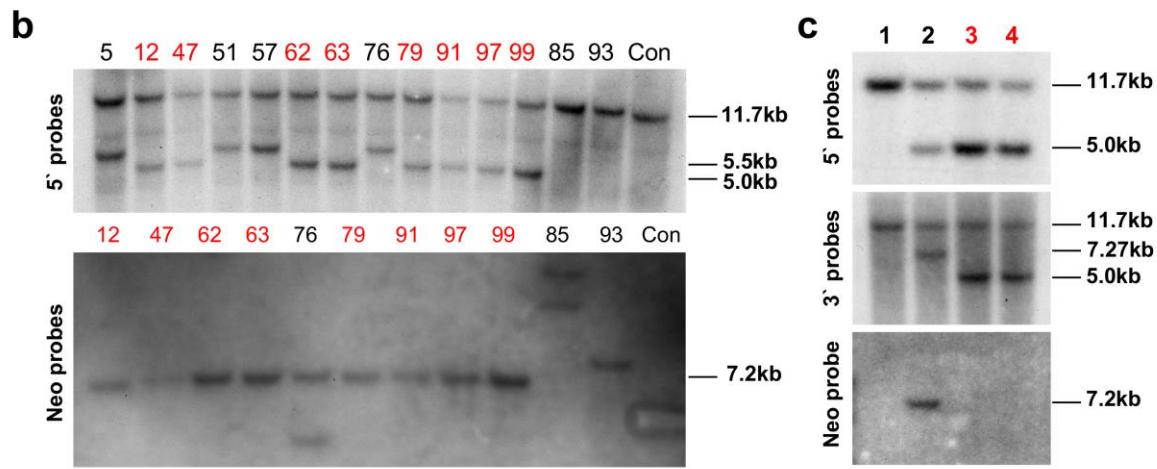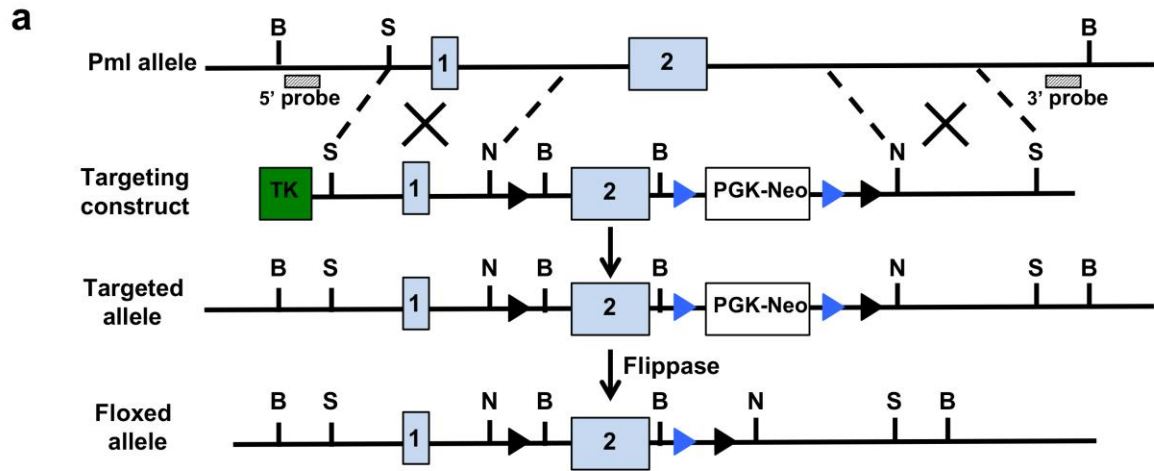
Supplementary Figure 2

Generation of *Pml*^flox/flox^ mice

(**a**) Schematic map of the WT *Pml* locus (top), targeting vector (upper middle) and predicted targeted allele (lower middle) and floxed allele (bottom). The *Pml* genomic sequence was cloned and inserted into the pEZ-LOX-FRT-DT vector. Black triangles mark the location of loxP sites that were utilized to excise the exon 2. Blue triangles mark the location of FRT sites that were utilized to excise the neomycin resistant cassette. The probes for Southern blot analysis are indicated (5′ and 3′ probes). *BamH*I digestion of genomic DNA from targeted ES cells was use to distinguish WT and targeted allele. *BamH*I (B), ScaI (S), *Not*I (N). (**b**) Southern blot analysis of recombined ES cell clones after digestion with *BamH*I and hybridization with the 5' probe (upper panel) and the neomycin (lower panel) probe. ES cell clones with corrected homologous recombination

are highlighted in red. (**c**) Southern blot analysis of tail DNA from F2 mice after digestion with *BamH*I and hybridization with the 5' probe (top), 3' probe and neomycine probe (bottom). The mice with deletion of neomycin resistant cassette are highlighted in red.
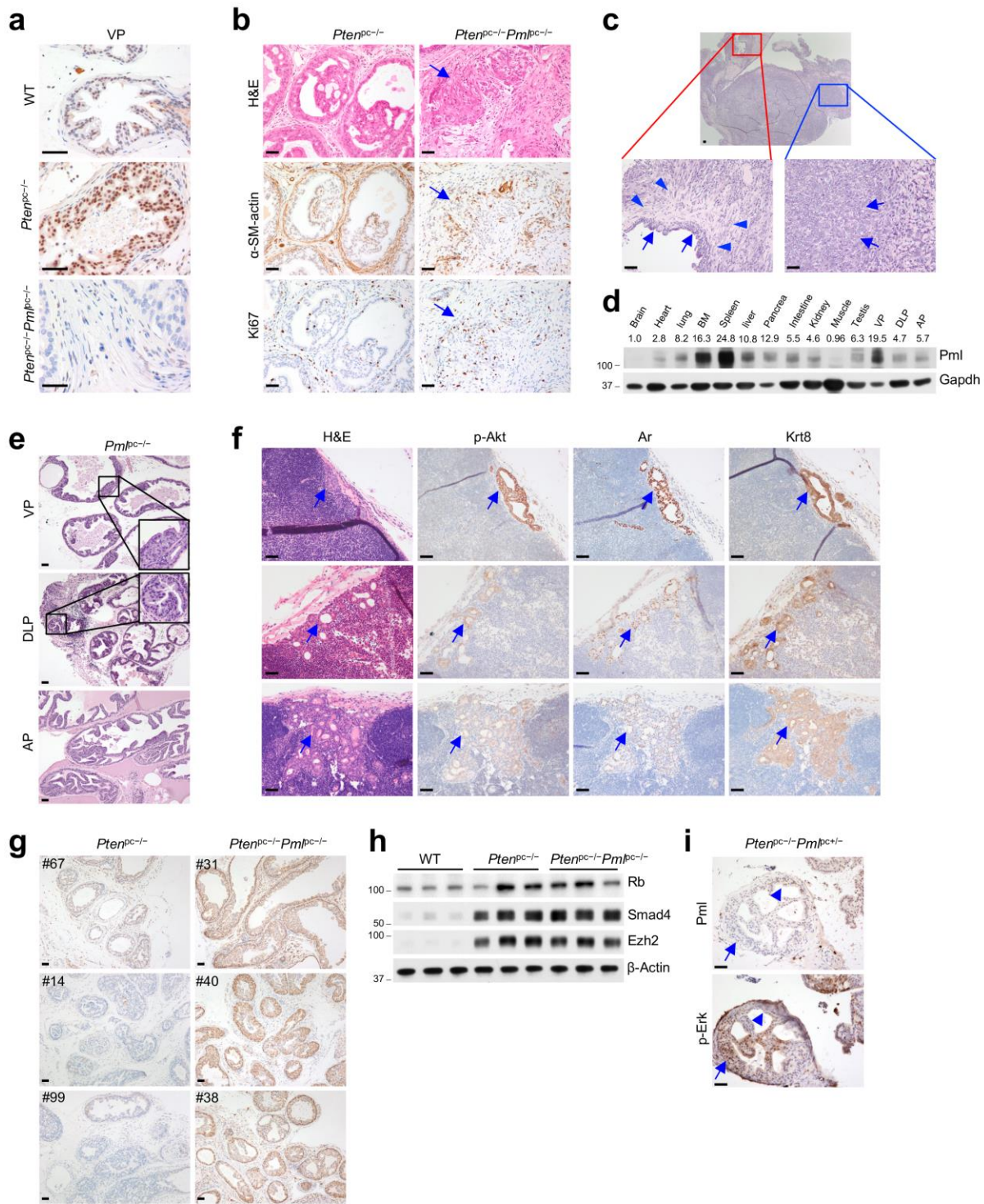
Supplementary Figure 3

Pml loss drives MAPK reactivation and metastatic progression in *Pten*-null CaP

(**a**) IHC staining for Pml in the VP tissues from WT, *Pten*^pc−/− and *Pten*^pc−/−*Pml*^pc−/− mice at 12 weeks of age. (**b**)

H&E and IHC staining of the DLP tissues from *Pten*^pc−/− and *Pten*^pc−/−*Pml*^pc−/− mice at 20 weeks of age. Note

that tumors in $Pten^{pc-/-}Pml^{pc-/-}$ mice acquired invasive feature. Invasiveness was confirmed by the absence of SM-α-actin staining along with high level of Ki67 staining in the cancer cells. Arrows indicate invasive cancer. (**c**) Higher magnification of $Pten^{pc-/-}Pml^{pc-/-}$ tumors at 13 months of age showing predominate adenocarcinoma (arrows) in the presence of focal features of sarcomatoid carcinoma with high-grade pleomorphic spindle cells (arrowheads). (**d**) IB analysis of tissue lysates for Pml from a WT mouse. (**e**) H&E-stained low-grade PIN in the VP and DLP tissues from a $Pml^{pc-/-}$ mouse at 12 months of age. Insets show crowding cells with large nuclei. (**f**) H&E and IHC staining of lumbar lymph node metastases from three $Pten^{pc-/-}Pml^{pc-/-}$ mice. Arrows indicate metastases. (**g**) IHC staining for phosphor-ERK in the DLP tissues from three pairs of $Pten^{pc-/-}$ and $Pten^{pc-/-}Pml^{pc-/-}$ mice at 12 weeks of age. (**h**) IB analysis of the DLP tissue lysates from WT, $Pten^{pc-/-}$ and $Pten^{pc-/-}Pml^{pc-/-}$ mice at 12 weeks of age. (**i**) IHC staining for Pml and phosphor-ERK in the DLP tissues from a $Pten^{pc-/-}Pml^{pc+/-}$ mouse at 12 weeks of age. Arrows indicate areas with lower level of Pml, but higher level of p-ERK. Arrowheads indicate areas with higher level of Pml, but lower level of p-ERK. Scale bars in all panels, 50μm. Uncropped images in **d** and **h** are shown in **Supplementary Fig. 7**.
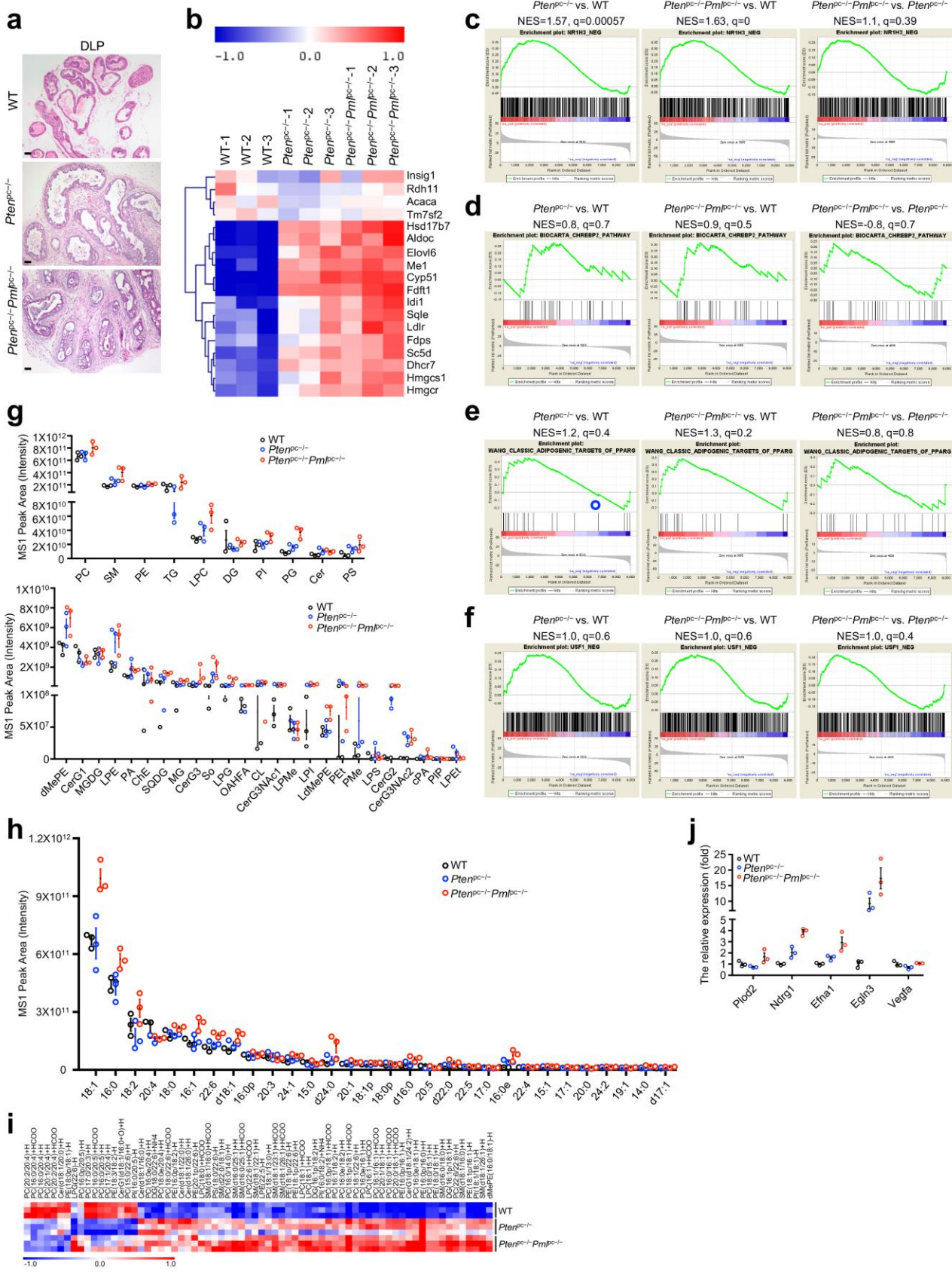
Transcriptome and lipidomics profiling of WT, *Pten*$^{pc-/-}$ and *Pten*$^{pc-/-}$*Pml*$^{pc-/-}$ prostates

(**a**) Representative H&E staining of DLP from WT, *Pten*$^{pc-/-}$ and *Pten*$^{pc-/-}$*Pml*$^{pc-/-}$ mice at 12 weeks of age. Scale bar, 50μm. (**b**) Heat map of the SREBP targets in the microarray analysis of prostate tissues from the three genotypes of mice. (**c-f**) GSEA enrichment plot for the targets of *LXR*, *ChREBP*, *PPARγ*, and *USF*. The up- to down-regulated genes from the ranked gene list were analysed with the GSEA algorithm for enrichment of all gene sets in MSigDB among WT, *Pten*$^{pc-/-}$ and *Pten*$^{pc-/-}$*Pml*$^{pc-/-}$ prostates. (**g,h**) The relative intensity of all the identifiable 35 lipid classes (**g**) or the 30 most abundant fatty acyl chains (**h**) in prostate tissues from the three genotypes of mice. (**i**) Heat map of the top 70 most regulated lipid ions in prostate tissues from the three genotypes of mice. (**j**) The validation of the expression changes of hypoxia-induced target genes by the qPCR among WT, *Pten*$^{pc-/-}$ and *Pten*$^{pc-/-}$*Pml*$^{pc-/-}$ prostates. Data shown in **g**, **h** and **j** are mean ± s.e.m.
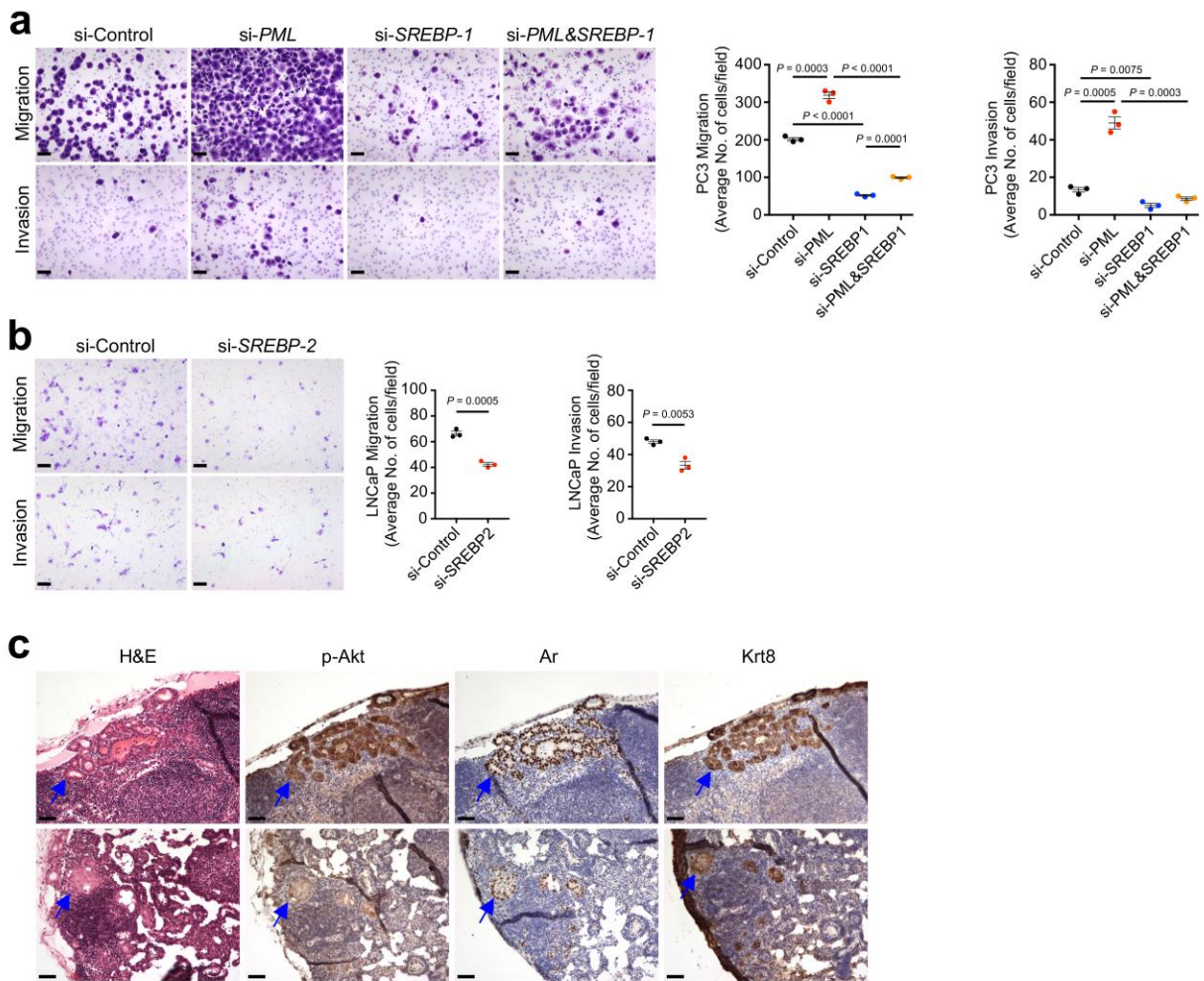
Supplementary Figure 5

SREBP-dependent lipogenesis is critical for *PML*-loss-induced CaP growth and metastasis

(**a**,**b**) Representative images and quantitation of migrated and invaded PC3 cells transfected with siRNA against PML or/and SREBP-1 (**a**), or LNCaP cells transfected siRNA against SREBP-2 (**b**), in the migration and invasion assays. CaP cells were transfected with control or indicated siRNA for 48 hrs. PC3 cells were then subjected to 24-hr migration and invasion assay, while LNCaP cells were subjected to 24-hr migration and 48-hr invasion assay. (**c**) H&E and IHC staining of metastases in the lumbar lymph node of two vehicle-treated *Pten*^pc−/−^*Pml*^pc−/−^ mice. Arrows indicate metastases. In **a** and **b**, the results of one representative experiment are shown (n=3). Data are from three independent cultures (4 fields per insert). Data shown are mean ± s.e.m. Student's t-test (two-tailed) was used to determine significance. Scale bars in all panels, 50μm.
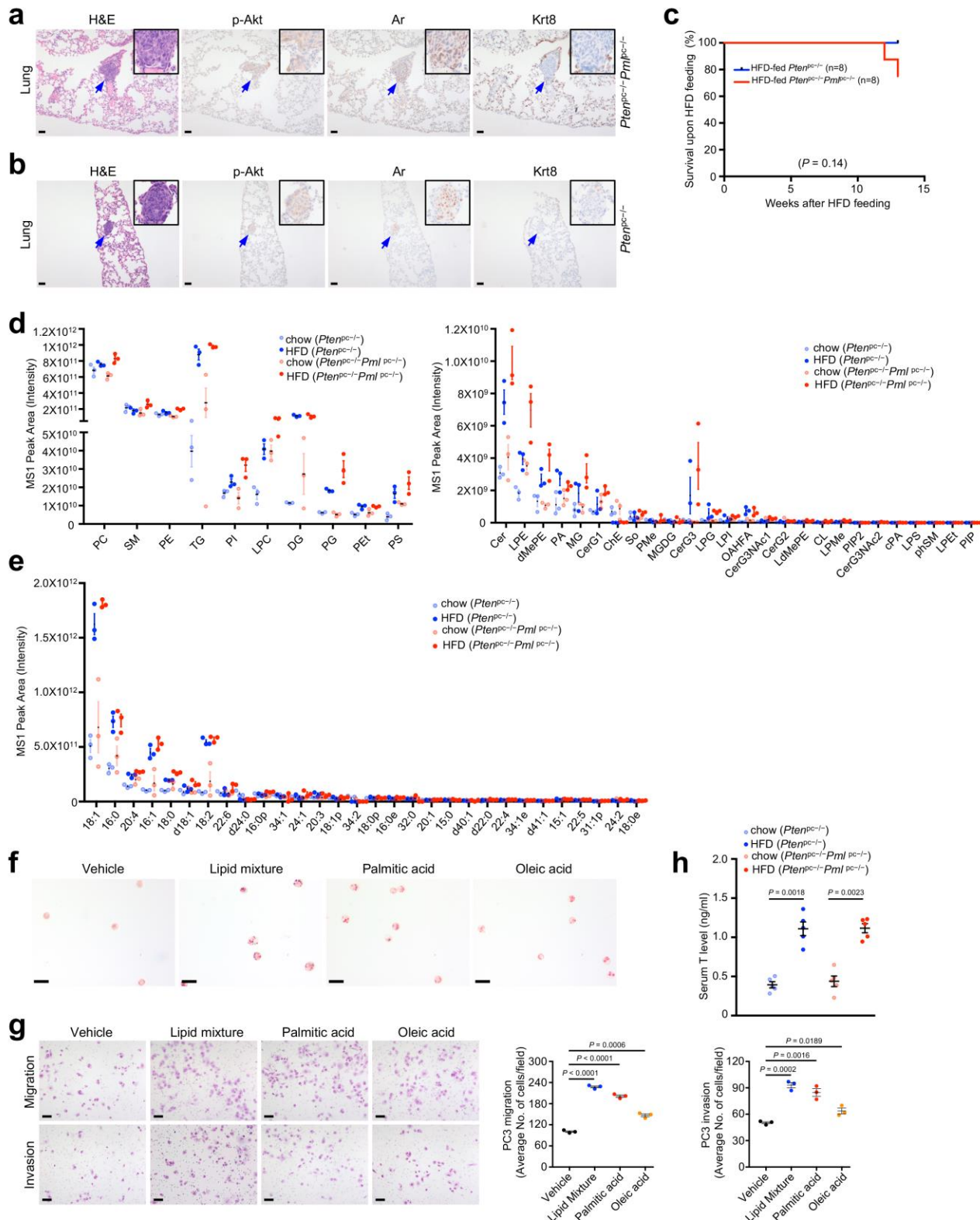
Supplementary Figure 6

A HFD drives metastatic progression in mouse models of CaP and increases lipid abundance in prostate tumors

(**a,b**) H&E and IHC staining of metastases in the lung of a representative $Pten^{pc-/-}Pml^{pc-/-}$ mouse (**a**) or a $Pten^{pc-/-}$ mouse (**b**). Arrows indicate metastases. (**c**) The survival analysis of $Pten^{pc-/-}$ and $Pten^{pc-/-}Pml^{pc-/-}$ mice upon 3-month HFD feeding beginning at 12 months of age. (**d,e**) The relative intensity of all the identifiable 36 lipid classes (**d**) or the 30 most abundant fatty acyl chains (**e**) in prostate tissues from chow- or HFD- fed $Pten^{pc-/-}$ and $Pten^{pc-/-}Pml^{pc-/-}$ mice. (**f**) The ORO staining of vehicle or dietary lipids treated PC3 cells. (**g**) Representative images and quantitation of migrated or invaded PC3 cells in the migration and invasion assay. PC3 cells were pretreated with BSA, 2% lipid mixture, BSA-conjugate palmitic acid or oleic acid for 7 days, then subjected to 24-hr migration and invasion assay. (**h**) The serum testosterone levels in chow- or HFD- fed $Pten^{pc-/-}$ and $Pten^{pc-/-}Pml^{pc-/-}$ mice at 14-15 months of age. In **g**, the results of one representative experiment are shown (n=5). Data are from three independent cultures (4 fields per insert). Data shown in **d**, **e**, **g** and **h** are mean ± s.e.m. Student's t-test (two-tailed) was used to determine significance. Scale bars in all panels, 50μm.
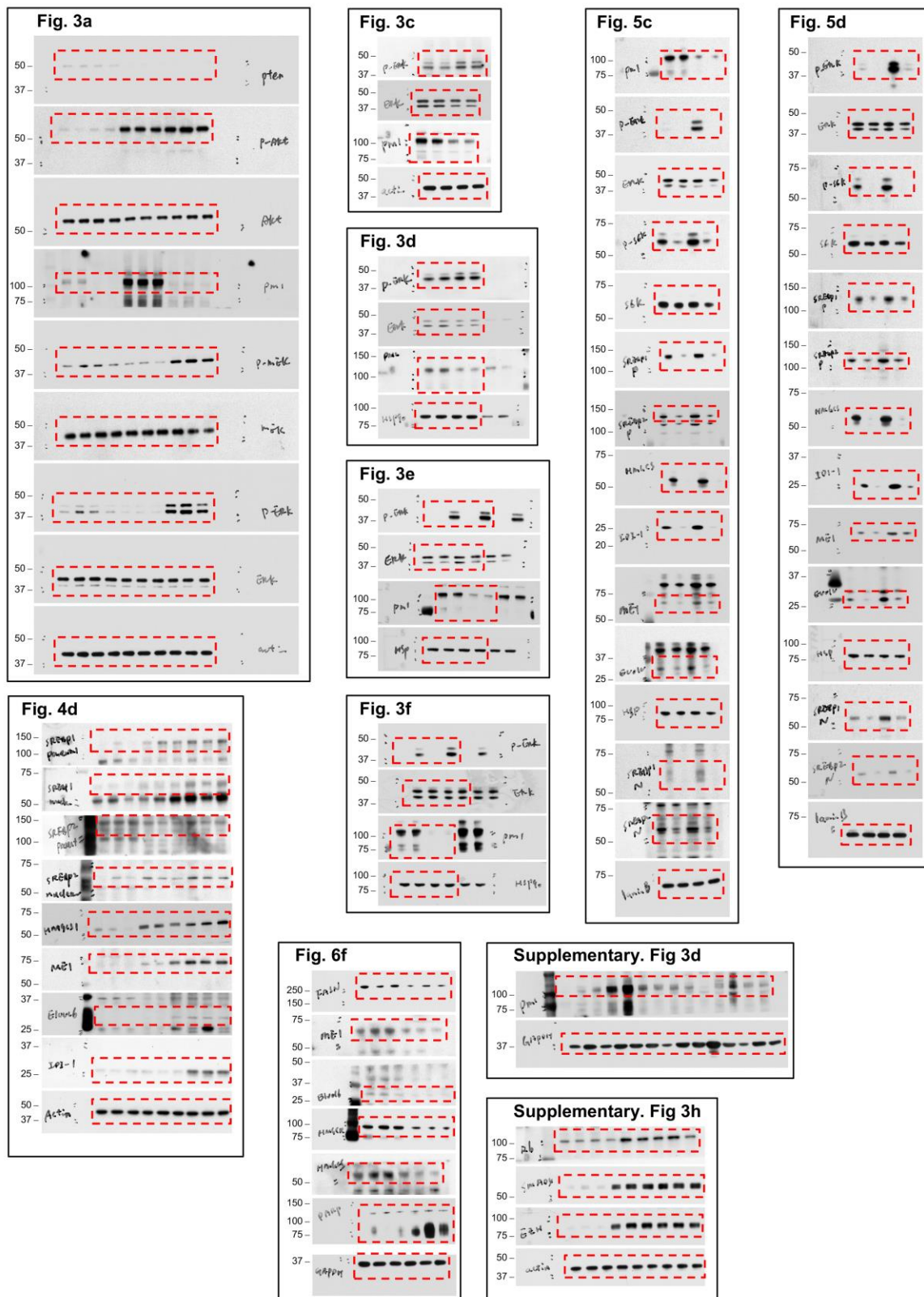
Supplementary Figure 7

Uncropped scans for the Western blot data.

Supplementary Table 8. Summary of fold change (Fc) and p value for the relative abundance of all the 35 lipid classes among the three genotypes of mice

	# of lipid Ions	$Pten^{pc-/-}$ vs. Wt		$Pten^{pc-/-}Pml^{pc-/-}$ vs. Wt		$Pten^{pc-/-}Pml^{pc-/-}$ vs. $Pten^{pc-/-}$	
		Fc	p-value	Fc	p-value	Fc	p-value
PG	90	1.98	<0.05	4.40	<0.01	2.22	<0.05
LPG	18	1.63	N.S.	6.94	<0.05	4.26	<0.05
MG	7	1.24	N.S.	2.84	<0.05	2.29	<0.05
LdMePE	3	1.07	N.S.	1.73	<0.05	1.62	<0.05
OAHFA	6	1.56	N.S.	2.27	<0.001	1.46	N.S.
PA	18	1.69	N.S.	1.58	<0.01	−1.07	N.S.
SQDG	2	1.99	N.S.	3.99	<0.01	2.00	N.S.
PE	213	1.04	N.S.	1.21	<0.05	1.15	N.S.
LPE	33	2.20	N.S.	2.38	<0.05	1.08	N.S.
dMePE	32	1.48	N.S.	1.75	<0.05	1.18	N.S.
LPC	90	1.43	N.S.	2.19	<0.05	1.53	N.S.
SM	106	1.40	N.S.	2.22	<0.05	1.58	N.S.
Cer	28	2.21	N.S.	1.93	<0.05	−1.15	N.S.
CerG2	4	42.56	<0.001	63.17	<0.01	1.48	N.S.
CerG3GNAc2	1	22.59	<0.01	23.55	<0.01	1.04	N.S.
LPI	9	3.65	<0.01	5.57	<0.05	1.53	N.S.
CerG3GNAc1	7	3.30	<0.05	2.97	<0.05	-1.11	N.S.
So	4	9.12	<0.05	18.93	<0.05	2.08	N.S.
cPA	3	26.33	<0.01	50.37	N.S.	1.91	N.S.
CL	39	5.20	<0.05	4.92	N.S.	−1.06	N.S.
PC	432	1.03	N.S.	1.21	N.S.	1.17	N.S.
TG	184	−1.80	N.S.	1.42	N.S.	2.55	N.S.
PS	137	2.75	N.S.	3.90	N.S.	1.42	N.S.
PI	124	1.14	N.S.	1.73	N.S.	1.52	N.S.
DG	90	−1.76	N.S.	−1.13	N.S.	1.55	N.S.
CerG1	14	−1.40	N.S.	−1.28	N.S.	1.09	N.S.
CerG3	12	2.25	N.S.	7.99	N.S.	3.55	N.S.
PMe	11	5.42	N.S.	19.27	N.S.	3.55	N.S.
ChE	9	1.68	N.S.	1.32	N.S.	−1.28	N.S.
PEt	7	9.45	N.S.	2.30	N.S.	−4.11	N.S.
LPEt	3	226.21	N.S.	69.40	N.S.	−3.26	N.S.
PIP	1	9.25	N.S.	7.51	N.S.	−1.23	N.S.
LPS	2	3.45	N.S.	−1.13	N.S.	−3.88	N.S.
MGDG	2	−1.10	N.S.	1.04	N.S.	1.14	N.S.
LPMe	2	−1.15	N.S.	−1.27	N.S.	−1.11	N.S.

Supplementary Table 9. Summary of fold change (Fc) and p value for the relative abundance of the 30 most abundant fatty acyl chains among the three genotypes of mice

| | $Pten^{pc-/-}$ vs. Wt | | $Pten^{pc-/-}Pml^{pc-/-}$ vs. Wt | | $Pten^{pc-/-}Pml^{pc-/-}$ vs. $Pten^{pc-/-}$ | |
	Fc	p-value	Fc	p-value	Fc	p-value
22:6	1.22	N.S.	1.66	<0.01	1.36	<0.01
18:1	−1.18	N.S.	1.45	<0.01	1.52	<0.05
24:1	1.26	N.S.	1.70	<0.01	1.35	<0.05
16:0	−1.27	N.S.	1.28	<0.05	1.33	<0.05
16:1	1.02	N.S.	1.69	<0.05	1.65	<0.05
14:0	1.00	N.S.	1.97	<0.05	1.96	<0.05
18:0	1.02	N.S.	1.22	N.S.	1.19	<0.05
18:1p	1.06	N.S.	1.33	<0.001	1.25	N.S.
d18:1	1.28	N.S.	1.69	<0.01	1.32	N.S.
20:1	1.11	N.S.	1.43	<0.05	1.29	N.S.
d16:0	1.70	N.S.	2.84	<0.05	1.67	N.S.
d17:1	1.24	N.S.	1.71	<0.05	1.38	N.S.
16:0e	3.26	<0.01	5.60	<0.05	1.72	N.S.
15:0	−1.67	<0.001	−1.06	N.S.	1.54	N.S.
20:5	−2.41	<0.001	−1.47	N.S.	1.64	N.S.
d22:0	1.49	<0.001	2.14	N.S.	1.44	N.S.
17:0	−1.72	<0.01	−1.15	N.S.	1.50	N.S.
18:2	−1.11	N.S.	1.37	N.S.	1.86	N.S.
20:4	−1.40	N.S.	−1.35	N.S.	1.08	N.S.
16:0p	1.03	N.S.	1.15	N.S.	1.12	N.S.
20:3	1.15	N.S.	−1.07	N.S.	−1.23	N.S.
d24:0	1.66	N.S.	3.54	N.S.	2.14	N.S.
18:0p	1.19	N.S.	1.17	N.S.	−1.02	N.S.
22:5	−1.12	N.S.	1.09	N.S.	1.20	N.S.
22:4	1.18	N.S.	1.26	N.S.	1.07	N.S.
15:1	1.28	N.S.	1.64	N.S.	1.27	N.S.
17:1	−1.24	N.S.	1.19	N.S.	1.48	N.S.
20:0	−1.60	N.S.	1.00	N.S.	1.60	N.S.
24:2	1.24	N.S.	1.40	N.S.	1.13	N.S.
19:1	−1.08	N.S.	1.13	N.S.	1.22	N.S.

Supplementary Table 13. Summary of fold change (Fc) and p value for the relative abundance of all the 36 lipid classes among chow- and HFD-fed mice

	# of lipid Ions	$Pten^{pc-/-}$ HFD vs. chow		$Pten^{pc-/-}Pml^{pc-/-}$ HFD vs. chow		chow $Pten^{pc-/-}Pml^{pc-/-}$ vs. $Pten^{pc-/-}$		HFD $Pten^{pc-/-}Pml^{pc-/-}$ vs. $Pten^{pc-/-}$	
		Fc	p-value	Fc	p-value	Fc	p-value	Fc	p-value
DG	196	10.00	<0.001	4.06	<0.01	2.38	N.S.	−1.03	N.S.
PG	105	2.96	<0.001	5.69	<0.01	−1.18	N.S.	1.63	N.S.
TG	332	22.15	<0.001	3.53	<0.05	7.02	N.S.	1.12	N.S.
PS	324	4.18	<0.01	2.02	<0.05	2.80	<0.01	1.35	N.S.
Cer	27	2.42	<0.01	1.32	<0.05	1.32	N.S.	1.33	N.S.
LPE	33	2.15	<0.01	1.98	<0.05	1.92	<0.01	1.76	N.S.
OAHFA	10	12.89	<0.01	4.30	<0.05	2.64	N.S.	−1.14	N.S.
PI	130	1.36	<0.05	2.28	<0.05	−1.20	N.S.	1.40	N.S.
PEt	20	1.81	<0.05	1.55	<0.05	1.17	N.S.	1.00	N.S.
dMePE	43	2.03	<0.05	3.58	<0.05	−1.23	N.S.	1.44	N.S.
LPC	137	2.53	<0.01	1.85	N.S.	2.47	<0.01	1.81	N.S.
LdMePE	5	7.08	<0.01	2.03	N.S.	7.35	N.S.	2.11	N.S.
LPEt	2	27.23	<0.01	3.28	N.S.	32.26	N.S.	3.89	<0.05
CerG3GNAc2	1	5.33	<0.05	2.66	N.S.	4.77	N.S.	2.38	N.S.
ChE	7	−147.0	<0.01	−28.53	N.S.	1.25	N.S.	6.45	N.S.
PE	246	1.18	N.S.	1.86	<0.001	−1.24	N.S.	1.27	<0.05
LPG	21	4.83	N.S.	5.74	<0.001	−1.03	N.S.	1.16	N.S.
PC	584	1.11	N.S.	1.35	<0.01	−1.11	N.S.	1.10	N.S.
MG	19	2.33	N.S.	3.16	<0.05	1.23	N.S.	1.67	N.S.
LPI	13	2.63	N.S.	1.73	<0.05	2.33	N.S.	1.53	N.S.
SM	134	−1.20	N.S.	1.71	<0.05	−1.43	N.S.	1.43	N.S.
SO	4	−1.07	N.S.	2.45	<0.05	−1.50	N.S.	1.75	N.S.
PA	4	2.43	N.S.	1.51	N.S.	1.35	N.S.	−1.20	N.S.
CerG1	7	1.63	N.S.	1.49	N.S.	1.88	N.S.	1.72	N.S.
PMe	12	−1.75	N.S.	4.79	N.S.	−3.05	N.S.	2.75	N.S.
MGDG	1	−2.42	N.S.	3.91	N.S.	−4.15	<0.05	2.28	N.S.
CerG3	13	12.87	N.S.	70.80	N.S.	−2.63	N.S.	2.09	N.S.
CerG3GNAc1	6	2.29	N.S.	1.31	N.S.	4.58	<0.05	2.62	<0.05
CerG2	6	2.79	N.S.	−1.62	N.S.	7.25	N.S.	1.61	N.S.
CL	12	2.98	N.S.	6.97	N.S.	1.66	N.S.	3.88	N.S.
PIP2	2	−3.81	N.S.	11.62	N.S.	−9.74	N.S.	4.54	N.S.
cPA	3	3.56	N.S.	7.73	N.S.	1.06	N.S.	2.30	N.S.
LPS	1	3.38	N.S.	3.61	N.S.	2.11	N.S.	2.25	N.S.
PIP	2	4.56	N.S.	40.27	N.S.	1.42	N.S.	12.50	N.S.
LPMe	2	−209.8	N.S.	–	–	–	–	–	–
phSM	1	–	–	–	–	6.82	N.S.	–	–

Supplementary Table 14. Summary of fold change (Fc) and p value for the relative abundance of the 30 most abundant fatty acyl chains among chow- and HFD-fed mice

	$Pten^{pc-/-}$ HFD vs. chow		$Pten^{pc-/-}Pml^{pc-/-}$ HFD vs. chow		chow $Pten^{pc-/-}Pml^{pc-/-}$ vs. $Pten^{pc-/-}$		HFD $Pten^{pc-/-}Pml^{pc-/-}$ vs. $Pten^{pc-/-}$	
	Fc	p-value	Fc	p-value	Fc	p-value	Fc	p-value
18:1	3.20	<0.001	2.66	<0.01	1.34	N.S.	1.11	N.S.
16:1	4.36	<0.001	3.13	<0.01	1.64	N.S.	1.18	N.S.
18:0	1.95	<0.001	1.64	<0.05	1.60	N.S.	1.35	<0.001
18:2	6.43	<0.001	3.09	<0.05	2.18	N.S.	1.05	N.S.
16:0	2.40	<0.01	1.78	<0.05	1.38	N.S.	1.02	N.S.
20:4	1.70	<0.01	1.36	<0.05	1.43	N.S.	1.14	<0.05
15:1	2.20	<0.05	3.04	<0.01	−1.25	N.S.	1.10	N.S.
22:5	1.43	<0.05	1.21	<0.05	1.65	<0.001	1.40	<0.05
31:1p	−2.35	<0.05	1.98	<0.001	2.22	<0.05	2.10	<0.01
d24:0	−4.05	<0.05	1.64	N.S.	−5.67	<0.05	1.17	N.S.
d40:1	−1.58	<0.05	−1.05	N.S.	−1.45	N.S.	1.02	N.S.
22:4	1.32	N.S.	1.98	<0.001	−1.21	N.S.	1.24	<0.05
34:1e	−1.03	N.S.	2.05	<0.001	−1.58	N.S.	1.34	N.S.
16:0e	1.34	N.S.	1.88	<0.01	−1.23	N.S.	1.14	N.S.
16:0p	−1.01	N.S.	1.74	<0.01	−1.24	N.S.	1.42	<0.05
18:1p	−1.06	N.S.	1.87	<0.01	−1.51	<0.01	1.31	N.S.
d18:1	1.33	N.S.	1.70	<0.05	1.11	N.S.	1.43	N.S.
20:3	1.73	N.S.	1.68	<0.05	−1.10	N.S.	−1.13	N.S.
20:1	1.05	N.S.	2.25	<0.05	−1.73	N.S.	1.25	<0.01
18:0e	−1.01	N.S.	3.15	<0.05	−2.37	<0.05	1.34	N.S.
22:6	1.02	N.S.	1.76	N.S.	−1.02	N.S.	1.68	N.S.
34:1	−1.20	N.S.	−1.39	N.S.	−1.38	<0.05	−1.59	N.S.
24:1	1.04	N.S.	2.04	N.S.	−1.10	N.S.	1.77	N.S.
34:2	−1073.2	N.S.	−284.8	N.S.	−3.39	N.S.	1.11	N.S.
18:0p	1.43	N.S.	1.37	N.S.	1.00	N.S.	−1.03	N.S.
32:0	1.21	N.S.	−1.63	N.S.	1.40	<0.05	−1.41	N.S.
15:0	1.05	N.S.	1.03	N.S.	1.18	N.S.	1.16	N.S.
d22:0	1.00	N.S.	1.66	N.S.	−1.12	N.S.	1.48	N.S.
d41:1	−1.71	N.S.	1.19	N.S.	−1.63	N.S.	1.25	N.S.
24:2	1.20	N.S.	1.20	N.S.	−1.90	N.S.	1.90	N.S.

Supplementary Table 15. Sequences of siRNAs used in this study

Names	Sequences of siRNAs
h-PML-siRNA1	5'-GCAACCAGUCGGUGCGUGA-3'
h-PML-siRNA2	5'-CCGACUUCUGGUGCUUUGA-3'
h-SREBP1-siRNA1	5'-CGGAGAAGCUGCCUAUCAA-3'
h-SREBP1-siRNA2	5'-CCGUGUACUUCUGGAGGCA-3'
h-SREBP2-siRNA1	5'-CAGAGUUCCUUCUGCCAUU-3'
h-SREBP2-siRNA2	5'-GUGUGAUUGUCCUGAGCGU-3'
siGENOME Non-Targeting siRNA #2	5'-UAAGGCUAUGAAGAGAUAC-3'

Supplementary Table 16. Sequences of q-PCR primer used in this study

	Sequence of Primers
Mouse *Ldlr*	Forward: 5'-CAAGAGGCAGGGTCCAGA-3'
	Reverse: 5'-CCAATCTGTCCAGTACATGAAGC-3'
Mouse *Hmgcr*	Forward: 5'-GGCCTCCATTGAGATCCG-3'
	Reverse: 5'-CACAATAACTTCCCAGGGGT-3'
Mouse *Hmgcs1*	Forward: 5'-GGTCTGATCCCCTTTGGTG-3'
	Reverse: 5'-TTCAAAGGAAGTGACCCAGG-3'
Mouse *Elovl6*	Forward: 5'-GCAAAGCACCCGAACTAGG-3'
	Reverse: 5'-GAGCACAGTGATGTGGTGGT-3'
Mouse *Me1*	Forward: 5'-GACGCCTTCCTGGATGAGT-3'
	Reverse: 5'-ATCTTCAAACTGAATAAGGCAATTC-3'
Mouse *Hsd17b7*	Forward: 5'-CATAATGTGGCTCCTTCGCT-3'
	Reverse: 5'-AGAGACTCCGGTTTTTGGTG-3'
Mouse *Idi1*	Forward: 5'-GAGTTGGGAATACCCTTGGA-3'
	Reverse: 5'-TCAACTTCATGTTCACCCCA-3'
Mouse *Plod2*	Forward: 5'-GAGAGGCGGTGATGGAATGAA-3'
	Reverse: 5'-ACTCGGTAAACAAGATGACCAGA-3'
Mouse *Ndrg1*	Forward: 5'-ATGTCCCGAGAGCTACATGAC-3'
	Reverse: 5'-CCTGCTCCTGAACATCGAACT-3'
Mouse *Egln3*	Forward: 5'-AGGCAATGGTGGCTTGCTATC-3'
	Reverse: 5'-GCGTCCCAATTCTTATTCAGGT-3'
Mouse *Efna1*	Forward: 5'-CTTCACGCCTTTTATCTTGGGC-3'
	Reverse: 5'-TGGGGATTATGAGTGATTTTGCC-3'
Mouse *Vegfα*	Forward: 5'-ATCTTCAAGCCGTCCTGTGT-3'
	Reverse: 5'-GCATTCACATCTGCTGTGCT-3'
Mouse *Sdha* (Internal control)	Forward: 5'-GCTCCTGCCTCTGTGGTTGA-3'
	Reverse: 5'-AGCAACACCGATGAGCCTG-3'
Human *LDLR*	Forward: 5'-CTACAAGTGGGTCTGCGATG-3'
	Reverse: 5'-TTTGCAGGTGACAGACAAGC-3'
Human *HMGCR*	Forward: 5'-GTTCGGTGGCCTCTAGTGAG-3'
	Reverse: 5'-GCATTCGAAAAAGTCTTGACAAC-3'
Human *HMGCS1*	Forward: 5'-TTCGTGGCTCACTCCCTTT-3'
	Reverse: 5'-CTGTCACTGTTTCCTCCTTCG-3'
Human *ELOVL6*	Forward: 5'-CAAAGCACCCGAACTAGGAG-3'
	Reverse: 5'-TGGTGATACCAGTGCAGGAA-3'
Human *ME1*	Forward: 5'-GCAGTGCTACAAAATAACCAAGG-3'
	Reverse: 5'-TGGAAGAGTGACTGGATCAAAA-3'
Human *HSD17B7*	Forward: 5'-AACAGGAACTTCAACCAGCAG-3'
	Reverse: 5'-GGCATCAACAGCGTCCATA-3'
Human *IDI1*	Forward: 5'-GCTAGGAATTCCCTTGGAAGA-3'
	Reverse: 5'-GTTCACCCCAGATACCATCAG-3'
Human *PML*	Forward: 5'-CGCCCTGGATAACGTCTTTTT-3'
	Reverse: 5'-CTCGCACTCAAAGCACCAGA-3'
Human *RPLP0* (Internal control)	Forward: 5'-GCTTCCTGGAGGGTGTCC-3'
	Reverse: 5'-GGACTCGTTTGTACCCGTTG-3'